



# MOVING THE AMBISONICS SWEET-SPOT BY ADAPTING LOUSPEAKER EQUALIZATION AND AMBISONICS DECODING

Matthieu Kuntz\*    Bernhard U. Seeber

Audio Information Processing, Technical University of Munich, Germany

## ABSTRACT

Virtual acoustic environments are becoming a widespread tool in hearing research. Free-field reproduction allows the design of more realistic experiments, where participants can turn their heads and move around without the need for individualized Head-related transfer functions or head tracking. A limitation of commonly used sound field synthesis techniques, in particular Ambisonics, is their decreasing accuracy with increasing distance from the center of the loudspeaker array. While participants can move around in the reproduced sound field, it is not possible to control the sound field they receive at off-center positions to the degree required for hearing research. In this work, we consider a two-dimensional 36-loudspeaker array, where the loudspeakers are typically equalized in the center of the array. We investigate the possibility of moving the Ambisonics sweet-spot by equalizing the loudspeakers at different points inside the loudspeaker array. Simulations show that at least 50% of the sweet-spot size is preserved when moving the equalization point. Adapting the relative loudspeaker positions for the Ambisonics decoding reduces the parallax shift observed in Ambisonics systems.

**Keywords:** *Virtual acoustic environment, loudspeaker array, higher-order Ambisonics, local sound field synthesis.*

\*Corresponding author: [matthieu.kuntz@tum.de](mailto:matthieu.kuntz@tum.de).

**Copyright:** ©2023 Kuntz & Seeber. This is an open-access article distributed under the terms of the Creative Commons Attribution 3.0 Unported License, which permits unrestricted use, distribution, and reproduction in any medium, provided the original author and source are credited.

## 1. INTRODUCTION

A well-known problem with higher-order Ambisonics (HOA) is the limited size of the reproduction sweet-spot, typically located around the center of the loudspeaker array. The sound field reproduction with wave-field synthesis (WFS) is not limited by a sweet-spot around the center. Still, it exhibits spatial aliasing artefacts over the whole reproduction area [1], which depend on the listener position and become prominent above 1 kHz for a loudspeaker spacing between 10 cm and 30 cm [2]. This has been shown to lead to coloration artefacts [3]. Further, it is still unclear how these artefacts affect hearing aid and cochlear implant performance.

For hearing research, allowing participants to move and walk around in the loudspeaker array enables the implementation of more realistic listening experiments. This requires an accurate sound field reproduction over an extended area or an accurate reproduction on a smaller area around the listener, not necessarily coinciding with the center of the loudspeaker array. Numerical approaches based on transfer function inversion [4, 5] offer that option, as the target region for which the sound field is optimized can be chosen arbitrarily. Other approaches built upon WFS aim at moving the area of correct reconstruction to different locations in the loudspeaker array, either by recomputing the loudspeaker driving functions based on a different circular harmonics expansion center (Local WFS by Spatial Band-limitation, [6]) or by creating a virtual loudspeaker array at ideal positions around the desired target location and driving the virtual loudspeakers with conventional WFS (Local WFS by Virtual Secondary Sources, [7]). These approaches are derived analytically in the frequency domain.

The approach we propose consists of applying equalization filters to the individual loudspeakers to virtually move the

loudspeaker array with the listener. The change in loudspeaker equalization filters can be handled in the time domain by convolution software or embedded into the room impulse responses generated by a room simulation and auralization software, *e.g.*, the real-time Simulated Open Field Environment (rtSOFE [8]). The following work presents simulated results using horizontal loudspeakers of the Simulated Open Field Environment in the anechoic chamber at the Technical University of Munich [9], consisting of 36 loudspeakers in  $10^\circ$ -spacing.

## 2. METHODS

### 2.1 Sound field simulation

A virtual point source emitting a 2 kHz tone was placed at  $13^\circ$  azimuth and 4 m distance from the center of the loudspeaker array and reproduced using 17<sup>th</sup>-order HOA. A numerical simulation of the sound field resulting from the calculated loudspeaker signals was implemented in the time domain. The loudspeakers were modeled as omnidirectional point sources. We simulated the reproduced sound field on an area of 3 m by 3 m around the center of the loudspeaker array with a spatial resolution of 2 cm, resulting in a 151 by 151 points grid.

### 2.2 Loudspeaker driving functions

The loudspeaker driving functions are computed by combining two components: gains derived with HOA and a short equalization filter.

The loudspeakers were equalized on a single point inside the loudspeaker array. We defined a total of 25 equalization points, set on a 5 by 5 points grid spanning from -1 m to 1 m in both  $x$  and  $y$  directions, which were individually evaluated. The equalization of the loudspeakers was carried out by the scaling and resampling of a sinc pulse. This changes the amplitude and time of arrival (on a sub-sample basis) to compensate for the differences in level and time of arrival due to the distance from the loudspeaker to the individual equalization point. For real-life systems, an additional equalization to a flat frequency and linear phase response is needed to ensure an accurate sound field reproduction. We do not employ this additional equalization as the loudspeakers are simulated as perfect point sources.

The Ambisonics gains were computed using the *basic* decoder, as described in [10]. We considered two definitions for the loudspeaker angles in the decoding stage. The first angle definition corresponds to the loudspeaker angles at the center of the loudspeaker array ( $0^\circ$ ,  $10^\circ$ , ...,  $350^\circ$ ) without considering the loudspeaker equalization

position. The second angle definition uses the loudspeaker angles relative to the current equalization position to reflect the angle change introduced by a translation of the equalization position. We refer to those definitions as position-dependent and position-independent Ambisonics decoding. The driving functions were also normalized at each individual equalization position to compensate for the level changes introduced by the deviation from the ideal loudspeaker arrangement when using position-dependent loudspeaker angles in the Ambisonic decoding, a phenomenon described in [10].

### 2.3 Evaluation metrics

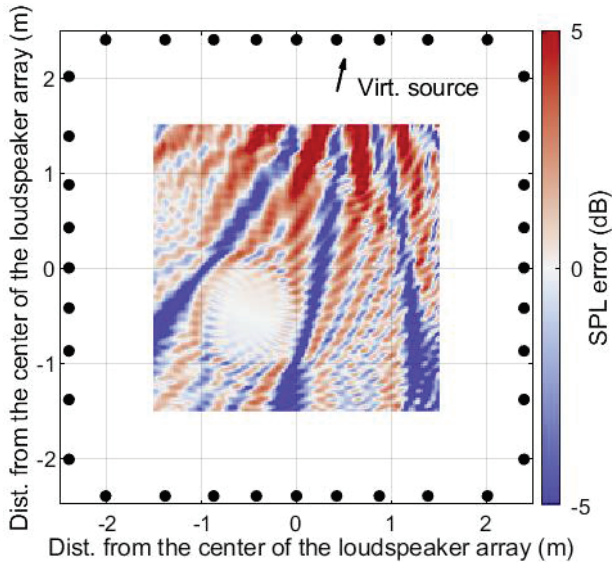
The sound pressure level and the direction of the sound pressure gradient were computed from the simulated sound field. The reference sound field used to compute the sweet-spot size is the theoretical sound field generated by a point source at  $13^\circ$  azimuth and 4 m distance, normalized to a level of 65 dB SPL at each individual loudspeaker equalization point. The sweet-spot was defined as the smallest distance from the loudspeaker equalization point where the sound pressure level error surpasses 2 dB.

## 3. RESULTS

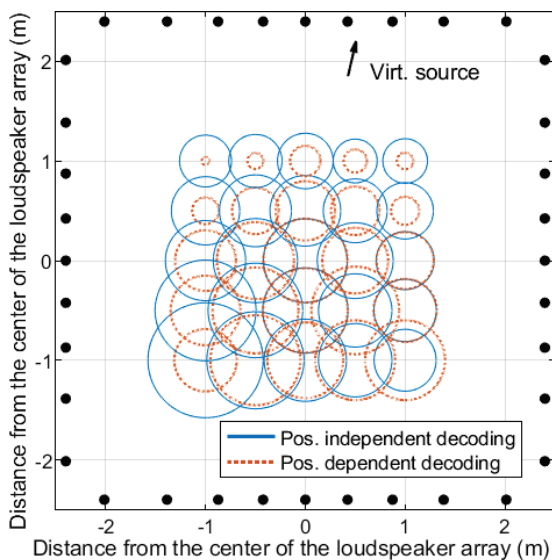
### 3.1 Sound pressure level

Figure 1 shows the sound pressure level error over the whole evaluation area for an equalization position at  $(-0.5, -0.5)$  m from the center of the loudspeaker array. The sweet-spot is about 40-50 cm in radius, framed by two bands of destructive interferences quite typical for the HOA *basic* decoder in anechoic conditions [11].

To easily compare different loudspeaker equalization positions and the different loudspeaker angle definitions, Figure 2 only shows the sweet-spot radius. For the position-independent loudspeaker angles, the sweet-spot radius increases with increasing distance from the virtual sound source, going from 22 cm at the equalization position  $(0.5, 1)$  m to 58 cm at the bottom left corner. These radii correspond to 52% and 137% of the sweet-spot radius in the center, respectively. For position-dependent loudspeaker angles, the sweet-spot sizes are, in general, smaller, the exceptions being three equalization points on the bottom right corner:  $(1, -1)$ ,  $(0.5, -1)$  and  $(0.5, -0.5)$ . Figure 2 shows that the sweet-spot can be translated to areas far away from the original sweet-spot around the center of the loudspeaker array.



**Figure 1.** Sound pressure level error at the loudspeaker equalization position (-0.5,-0.5). The black dots indicate the loudspeaker positions, the arrow points towards the virtual source at 4 m distance and 13° azimuth.



**Figure 2.** Sweet-spot size in meters represented by a circle around the respective loudspeaker equalization position. The black dots indicate the loudspeaker positions, the arrow points towards the virtual source at 4 m distance and 13° azimuth.

### 3.2 Gradient direction of the sound pressure field

Figure 3 shows the sound pressure gradient direction observed for different loudspeaker equalization positions. The position-independent loudspeaker angles show larger changes in the gradient direction, indicating a larger change in wave front direction when changing the loudspeaker equalization position. They are oriented towards the 10° loudspeaker, which contributes the most to the reproduced sound field, instead of the virtual sound source. This creates the parallax shift observed in HOA due to the distance mismatch between the virtual and the physical sources. The position-dependent loudspeaker angles show a relatively constant direction, close to the 13° observed in the center, except for the equalization points at the top left and right corners, with -7° and 22°, respectively.

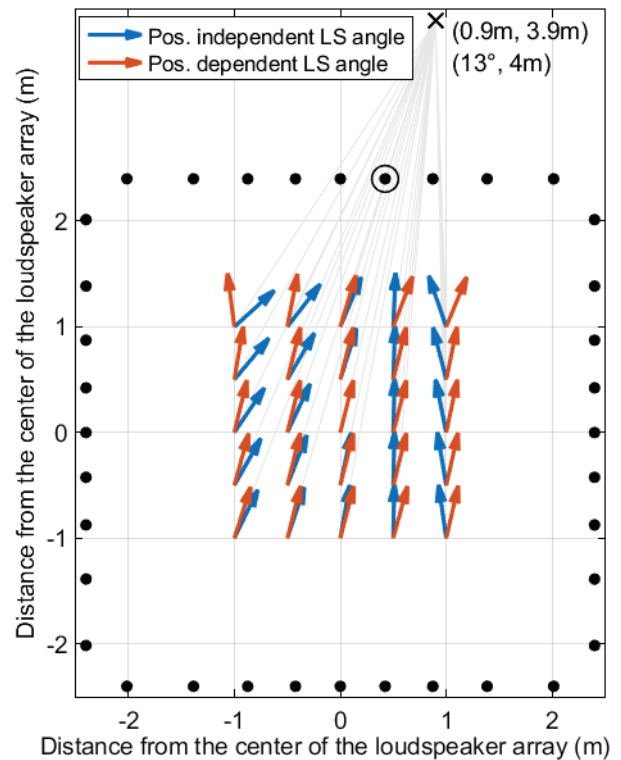


**Figure 3.** Sound pressure gradient direction for different loudspeaker equalization positions. The black dots indicate the loudspeaker positions, the grey lines serve as a visual aid to compare the gradient directions to the directions of the virtual source, marked by a black cross. The circled loudspeaker corresponds to the 10° loudspeaker.

Since position-dependent Ambisonic decoding changes the loudspeaker gains depending on the equalization position, the 10° loudspeaker is no longer the main contributor to the reproduced sound field, thus compensating the parallax shift. However, this comes at the cost of reduced sweet-spot size, especially further away from the center.

#### 4. DISCUSSION

Changing the point in the loudspeaker array for which the loudspeakers are equalized enables the translation of the Ambisonics sweet-spot, which we derived from the sound pressure level of the reproduced sound field. With the position-independent Ambisonics decoding, the sweet-spot is always larger than a human head, which should provide ear signals with error <2 dB and thus accurate enough for many applications in hearing research. Whether the parallax shift is problematic depends on the application. When the loudspeaker angles for the Ambisonics decoding are adapted to the equalization position, the parallax shift is strongly reduced at the expense of a smaller sweet-spot radius. However, it is still larger than 20 cm for all positions except the top row ( $y=1$  m) and the edge positions for  $y=0.5$  m, still allowing for decent listener movement.

#### 5. CONCLUSION

The proposed approach enables the translation of the Ambisonics sweet-spot in a loudspeaker array by adapting the position in the array on which the loudspeakers are equalized. Simulations show that the sweet-spot size around the new loudspeaker equalization position is at least 22 cm large at 2 kHz, effectively enabling correct reproduction at off-center positions, which was not the case with the basic HOA approach equalized in the center. Adapting the Ambisonic decoding can compensate for the parallax shift introduced by translating the sweet-spot. It can be integrated into other real-time FIR-filter-based processing with minimal computational overhead.

The ability to correctly reproduce the sound field at off-center positions, even at higher frequencies, is beneficial for listening experiments involving a moving listener.

#### 6. ACKNOWLEDGMENTS

The SOFE system was financed by the BMBF Bernstein Center for Computational Neuroscience, 01GQ1004B. This work was supported by TUM and the Deutsche Forschungsgemeinschaft (DFG, German Research Foundation) – Project ID 352015383 – SFB 1330 C5.

#### 7. REFERENCES

- [1] S. Spors, J. Ahrens, “A Comparison of Wave Field Synthesis and Higher-Order Ambisonics with Respect to Physical Properties and Spatial Sampling,” in *Proc. of the 125<sup>th</sup> AES Convention*, (San Francisco, CA, USA), pp. 7556, 2008
- [2] S. Spors, R. Rabensein, and J. Ahrens, “The Theory of Wave Field Synthesis Revisited,” in *Proc. of the 124<sup>th</sup> AES Convention*, (Amsterdam, The Netherlands), pp. 413–431, 2008
- [3] H. Wittek, “Perceptual differences between wavefield synthesis and stereophony,” PhD thesis, University of Surrey, 2007.
- [4] O. Kirkeby, P.A. Nelson, F. Orduna-Bustamante, and H. Hamada, “Local sound field reproduction using digital signal processing,” *The Journal of the Acoustical Society of America*, vol. 100, no. 3, pp. 1584–1593, 1996.
- [5] M. Kolundžija, C. Faller, and M. Vetterli, “Reproducing sound fields using MIMO acoustic channel inversion,” *Journal of the Audio Engineering Society*, vol. 59, no. 10, pp. 721–734, 2011.
- [6] N. Hahn, F. Winter, and S. Spors, “Local Wave Field Synthesis by Spatial Band-limitation in the Circular/Spherical Harmonics Domain,” in *Proc. of the 140<sup>th</sup> AES Convention*, (Paris, France), 2016.
- [7] S. Spors and J. Ahrens, “Local Sound Field Synthesis by Virtual Secondary Sources,” in *Proc. of the 40<sup>th</sup> AES International Conference*, (Tokyo, Japan), 2010.
- [8] B.U. Seeber and T. Wang, “real-time Simulated Open Field Environment (rtSOFE) software package (1.1),” Zenodo, DOI: 10.5281/zenodo.5648305, 2021.
- [9] B.U. Seeber and S.W. Clapp, “Interactive simulation and free-field auralization of acoustic space with the rtSOFE,” *The Journal of the Acoustical Society of America*, vol. 141, no. 5, pp. 3974, 2017.
- [10] F. Zotter and M. Frank: *Ambisonics: A Practical 3D Audio Theory for Recording, Studio Production, Sound Reinforcement, and Virtual Reality*, Springer Nature, 2019.
- [11] M. Kuntz, N. Kolotzek and B.U. Seeber, “Gemessener Schalldruckpegel im Lautsprecherarray für verschiedene Schallfeldsyntheseverfahren,” in *Fortschritte der Akustik - DAGA '21*, (Vienna, Austria), 2021.